NGU Report 2008.042

Structural mapping of the Åknes Rockslide, Stranda Municipality, Møre and Romsdal County, Western Norway

Geological Survey of Norway
NO-7441 Trondheim, Norway
Tel.: 47 73 90 40 00
Telefax 47 73 92 16 20

REPORT

Report no.: 2008.042 | ISSN 0800-3416 | Grading: Open

Title:
Structural mapping of the Åknes Rockslide, Møre and Romsdal County, Western Norway.

Authors:
Guri Venvik Ganerød

Client:
Åknes / Tafjord project

County:
Møre and Romsdal

Commune:
Stranda

Map-sheet name (M=1:250.000)
Berggrunnskart Ålesund

Map-sheet no. and -name (M=1:50.000)
1219 II Geiranger

Deposit name and grid-reference:
WGS 1984, UTM zone 32N - E 395821 N 6895249

Number of pages: 35 Price (NOK): 100,-
Map enclosures:

Fieldwork carried out:	Date of report:	Project no.:	Person responsible:
2005 - 2006	June 2008	309900	Jan S. Rønning

Abstract

Åknes is known as the most hazardous rockslide area in Norway at present, and is among the most investigated rockslides in the world, representing an exceptional natural laboratory. This study focuses on structural geology on five zones to interpret and understand the geometry of the rockslide area. The interpretations are further used to build a geological model of the site. This is a large rockslide with an estimated volume of 35-40 million m^3 (Derron et al., 2005), defined by a back scarp, a basal shear zone at about 50 meters depth and an interpreted toe zone where the sliding plane daylights the surface. This study resulted in a division of the central zone of the rockslide into four sub-domains, experiencing extension in the upper part and compression in the lower part. Structural mapping of the area indicates that the foliation of the gneiss plays an important role in the development of this rockslide. The upper boundary zone of the rockslide is seen as a back scarp that is controlled by, and parallel to, the pre-existing, steep foliation planes. Where the foliation is not favourably orientated in regard to the extensional trend, the back scarp follows a pre-existing fracture set or forms a relay structure. The foliation in the lower part, dipping 30° to 35° to S-SSE, seems to control the development of the basal sliding surface with its subordinate low angle trusts surfaces, which daylights at different levels. The sliding surfaces are sub-parallel to the topographic slope and are located along mica-rich layers in the foliation. Geophysical investigations which are important for the understanding of this rockslide are given in NGU reports 2006.002, 2007.026 and 2008.030. Results from this study are published in:
Ganerød, G.V., Grøneng, G., Rønning, J.S., Dalsegg, E., Elvebakk, H., Tønnesen, J.F., Kveldsvik, V., Eiken, T., Blikra, L.H. and Braathen, A., 2008. Geological model of the Åknes Rockslide, western Norway. Engineering Geology. http://dx.doi.org/10.1016/j.enggeo.2008.01.018

Keywords:	Structural geology	Åknes/Tafjord project
	Surface mapping	
	Rockslide	

CONTENTS

FIGURES

TABLES

APPENDIX

List of all localities with coordinates and description.

1. INTRODUCTION

Unstable rock slopes pose a threat to the inhabitants along Norwegian fjords, where prehistoric and historic rock avalanches have created tsunamis, some causing severe casualties (Blikra et al., 2005a). The site presented, Åknes, is located in western Norway (Figure 1). This is a large rockslide with an estimated volume of 35-40 million m^3 (Derron et al., 2005), defined by a back scarp, a basal shear zone at 50 metres depth and a toe zone where the basal sliding surface daylights the surface. Continuous creep of the rock mass and the fact that Åknes is situated above the fjord and in the vicinity of several communities as well as one of Norway's most visited tourist attractions (the Geirangerfjord, listed on the UNESCO`s World heritage list), have triggered a comprehensive investigation program. The overall aim of the project is firstly, to assess the likelihood that the rockslide will accelerate into a rock avalanche and secondly, to establish an early warning system with direct monitoring of deformation (translation and rotation), so that the local communities are able to evacuate in time.

Recent regional studies of the area are summarized in Braathen et al. (2004), Blikra et al. (2005a, b), Hermanns et al. (2006), Henderson et al. (2006) and Roth et al. (2006). Henderson et al. (2006) suggest that existing structures in the bedrock, such as foliation, faults and fracture zones, are controlling the development of the rockslides that occur in the fjord system. Where the foliation and slope angle coincide and structural weaknesses are favourably oriented, the rockslide hazard is considered greater (Henderson et al., 2006). Historical data from Åknes reveals three moderately sized rockslide occurrences within a rather short time interval: in the years 1850-1900, 1940 and 1962 (Kveldsvik et al., 2006). Other recent studies from the Åknes area are presented by Derron et al. (2005), who give an estimate of size of the rockslide, and Kveldsvik et al. (2006) who present a brief summary of the investigations and the progress of the project, and analyses of the 100.000m^3 rockslide that occurred in 1962 (Kveldsvik et al., 2007).

Despite the number of regional and local studies, a detailed structural understanding of the rockslide area is missing. A key issue has been to locate the basal sliding surface of the rockslide, since this is a prerequisite for precise volume estimation. Location of the basal sliding surface will also lead to a better understanding of the sliding mechanism(s) of the unstable area. The ongoing survey of the area is comprehensive and includes borehole logging and monitoring, which will help constrain the location of the basal sliding surface or sliding zone more precisely and yield additional quantitative data regarding spatial and temporal sliding velocities. The aim of this study has been to describe the rockslide area at Åknes by means of detailed structural surface mapping,

Results from the study show that there are structural limits to the rockslide area, consisting of the extensional back scarp zone at the top, a steeply dipping, NNW-SSE trending strike slip fault as the western boundary zone, a gentle dipping NNE-SSW trending pre-existing fault as the eastern boundary zone and a compressional toe zone at the bottom. The rockslide area is divided into four sub-domains (1 to 4), two mapped on the surface (2 and 4) and two mapped in the subsurface by geophysics (1 and 3, Figure 1). The sub-domains are bound by the basal

sliding surface with its four subordinate, low angle thrusts that stack the bedrock lobes upon one another, forming an imbricated thrust fan. The overall geometry is that of extension in the upper part and compression in the lower part of the slope. An outline of the rockslide is given in Figure 1b and c.

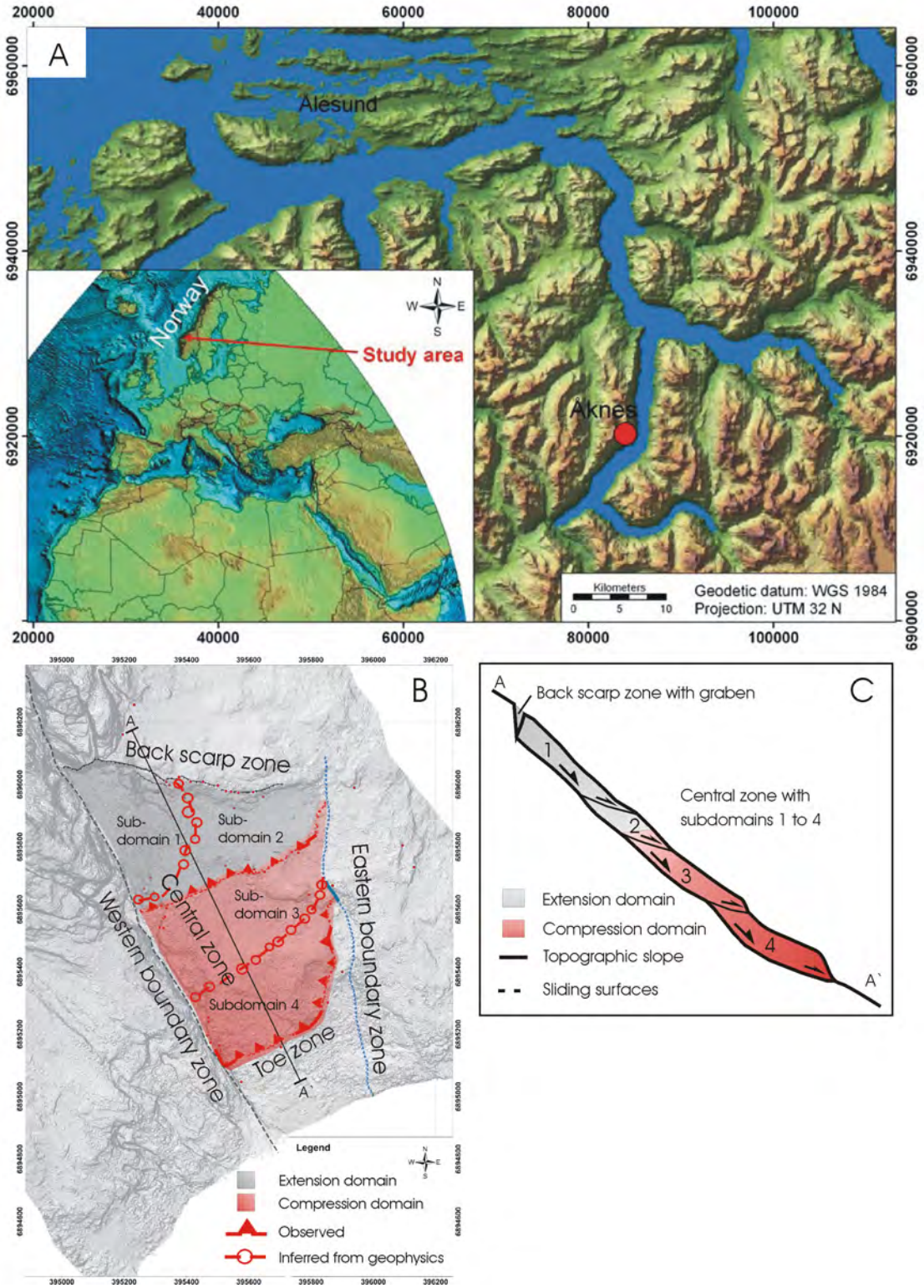

Figure 1: A) Location of the rockslide site of Åknes in western Norway. This site is found 150-900 metres above sea level in a SSE facing steep mountain slope. The main concern for this area is that a rock avalanche will reach the fjord at the foot of the slope, and trigger a tsunami in the fjord system. B) Map that locates domains and sub-domains (1, 2, 3 and 4) and key structures described in the text. C) Schematic profile (located in b) that outline domains, sub-domains and key structures (Ganerød et al., 2008).

2. GEOLOGICAL SETTING OF ÅKNES SITE

The Åknes rockslide is located in the Western Gneiss Region. The bedrock of the area is dominated by gneisses of Proterozoic age, which was altered and reworked during the Caledonian orogeny (Tveten et al., 1998). The gneisses have a magmatic origin and are described in the geological map sheet as undifferentiated gneisses that are locally migmatitic in composition, varying from quartz-dioritic to granitic (Tveten et al., 1998). Within certain areas the gneiss has a distinct metamorphic penetrative foliation (S_1, dominantly 080/30) that is folded around gently ESE-plunging axes (Tveten et al., 1998, Braathen et al., 2004). The bedrock at the study sites alters from a white to light pink, medium grained granitic gneiss to a dark grey biotite bearing granodioritic gneiss, and further to a subordinate white to light grey, hornblende to biotite bearing, medium grained dioritic gneiss. There are also laminae, and up to 20 cm thick layers, of biotite schist within the gneiss. All lithologies occur in layers parallel to the metamorphic foliation.

The Åknes site is a southward facing slope, with an average dip angle of 30-35°, with a topography that stretches from sea level to an elevation of 1300 metres over a distance of 1500 metres (Figure 1). Here, a subdivision of the rockslide area into five zones is proposed, based upon different structural signatures. The unstable area is estimated to be 800 metres across-slope and 1200 metres down-slope, with an upper boundary, the *Back Scarp Zone*, located 800-900 metres above sea level, and a lower boundary, the *Toe Zone*, at 150 metres above sea level. The western margin is a steep NNE-SSE trending strike slip fault, called the *Western Boundary Zone*, forming a narrow, deep crevasse in the mountainside (Figure 1). On the east side, the rockslide area is bound by a pre-existing fault dipping gently (35-45°) to the west, called the *Eastern Boundary Zone*. The fifth part of the rockslide is named the *Central Zone*.

3. METHODS

3.1 Structural mapping

Structural mapping is conducted on outcrops in the field, where fracture properties such as orientation, strike and dip with right hand rule (RHR) measurement (Figure 2a, Davis and Reynolds, 1996), length/persistence and frequency is collected. The fracture frequency is measured along a ruler in x direction parallel to foliation, y direction perpendicular to foliation, and if possible in a third direction (z) to estimate the block size. The foliation in gneissic rocks commonly represents a weakness in the bedrock and will therefore fracture along it, creating a higher fracture frequency in that direction as demonstrated in Figure 2b. This will give a dominance of fractures parallel to the foliation while other fracture orientations most likely are underrepresented in comparison. The data is later analysed per locality, for example as lower hemisphere stereographic projections (Wulff net) of fracture orientation (Figure 2a).

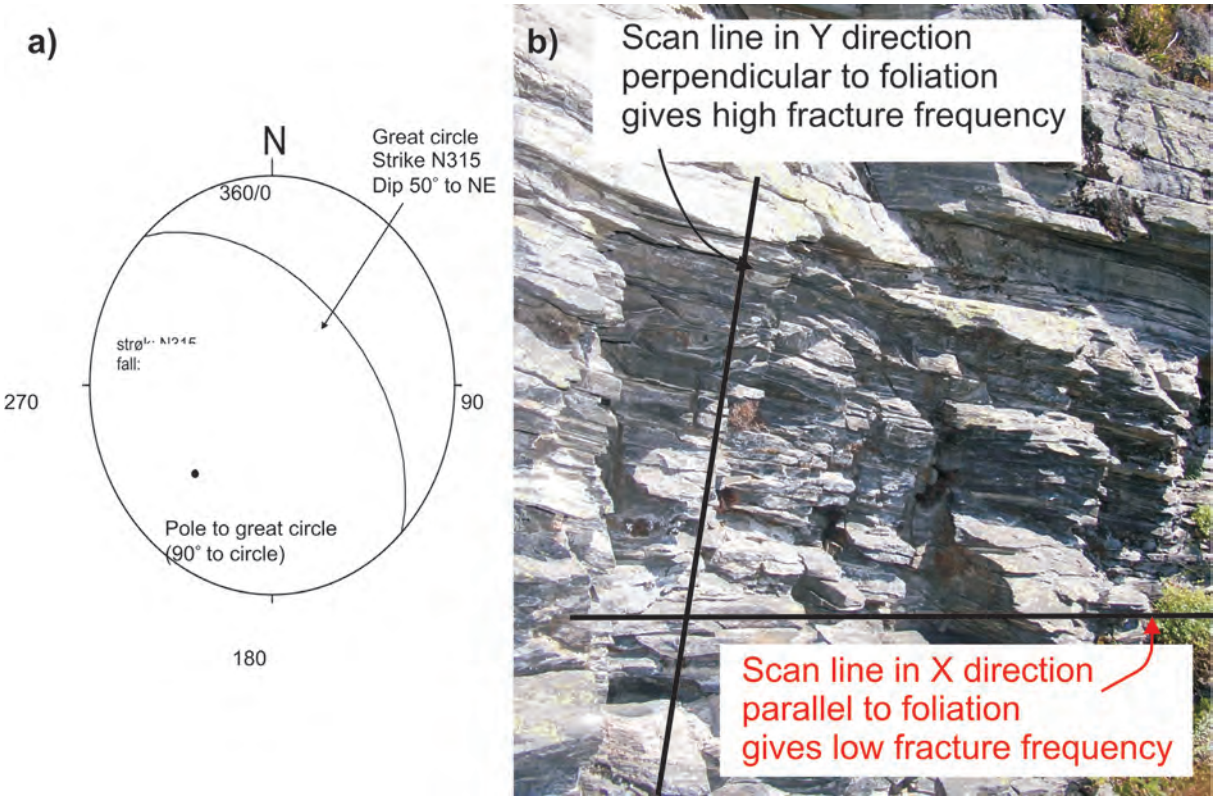

Figure 2: a) Stereographic projection with the Wulff net and Right Hand Rule measurement. Here a planar surface (fracture) is displayed with the orientation strike 315° and dip 50°, illustrated by a great circle and its coherent pole (90° to the great circle). This shows that the fracture has NW-SE strike and dip to NE. b) Example of how structural data such as fracture frequency is collected with the help of scan lines. Fracture frequency is collected in x direction parallel to foliation, in y direction perpendicular to foliation, and if possible in z direction to estimate the block size of the area. Fracture frequency collected in y direction gives commonly the highest value. From Ganerød et al. (2008).

3.2 Surface geophysical mapping

Geophysical methods such as Ground Penetrating Radar (GPR), refraction seismic and 2D resistivity profiling have been used to map the subsurface. The geophysical survey was performed by the Geological Survey of Norway. Several lines were measured in the rockslide area, of which parts will be presented here. The complete data collection is described in Rønning et al. (2006, 2007) and Elvebakk (2008). The 2D resistivity and GPR data were collected along the same profiles, while seismic acquisition was limited to three profiles (Rønning et al., 2006).

3.2.1

The GPR survey at the rockslide consists of seven profiles of altogether 5300 metres. One profile has NE-SW strike, four profiles are slope parallel with E-W strike, and two are oriented down-slope with N-S strike. The GPR profile presented has a total length of 250 metres with a NNW-SSE strike.

GeoRadar is an electro magnetic method that is used to detect structures in the subsurface (Reynolds, 1997). With an antenna electro magnetic pulses are sent into the subsurface, which are reflected off surfaces with different dielectric properties and received by a receiver antenna at the surface. The time of the propagating wave is recorded. This measurement is repeated with a fixed interval, giving a continuous image of the subsurface structures. The penetration depth and the resolution of the method depend on the signal frequency and the material property, such as electrical conductivity and dielectrisity. High antenna frequency (MHz) will give good data resolution but shallow penetration depths and visa versa. The GPR profiles were acquired using a frequency of 50 MHz and a shot point interval of 1 metre, with a GPR system called Sensors & Software Pulse EKKO 100. This gives reasonable resolution of the structures in the subsurface, but limits the penetration depths to about 30, and not more than 50, metres. The velocity analysis (processed CMP-gathers) performed in the area gave an average velocity to deep structures of 0.11 metres per nano-seconds (m/ns), which were used for depth conversion.

3.2.2 seismics

The seismic survey consists of one slope parallel profile with E-W strike and two down-slope profiles with ~N-S strike, totalling 1440 metres. The seismic profile presented has a total length of 420 metres with a NNW-SSE strike. For the seismic profiles the geophone spacing was 10 metres, with a total of 24 14 Hz vertical geophones depending on operator. Shot point interval was 30 to 300 metres with 100 to 600 grams of dynamite as energizer for each shot (Rønning et al., 2006).

The seismic method is based on the recording of first arrival times of P-wave travel time of waves in the subsurface. The wave propagates with the elasticity of the material, and the range of the seismic P-wave velocity calculated from the travel time of the wave, commonly range from 200 m/s up to above 6000 m/s. In fractured bedrock the seismic velocity is reduced dependent on fracture frequency, texture and filling (Reynolds, 1997). The refraction seismic is a method that is developed principally for mapping of horizontal layers, and is dependent upon there being an increase in velocity with depth. If a layer has lower velocity than the above laying layer, the seismic wave will not be refracted in the right manner, but continue in depth and gives rise to the phenomenon called a *hidden layer*. This layer is difficult to detect and may be interpreted as part of the above laying layer (Reynolds, 1997).

3.2.3 Resistivity

The 2D resistivity survey consists of eight profiles, one oriented NE-SW, five slope parallel with E-W strike, and two down-slope profiles with N-S strike, totalling about 10 000 metres. Here, a 420 metres long section out of an 1800 metre long down-slope profile is presented.

The resistivity method measures apparent resistivity (with unit Ωm) in the subsurface, which is a weighted average of all resistivity values within the measured volume (Reynolds, 1997, Dahlin, 1993). Measured apparent resistivities with different electrode configurations are converted into a true 2D resistivity profile through inversion (Loke, 2001). The 2D resistivity

profiles were acquired according to the Lund-system (Dahlin, 1993). Acquisition was collected with both Wenner and Dipol/Dipol configurations, with an electrode spacing of 10 metres for the shallow and 20 metres for the deeper parts of the profiles. In a few short profiles the electrode interval was reduced to 5 and 10 metres (Rønning et al., 2006). The depth penetration of the profile is approximately 130 metres, with reliable data coverage to approximately 70 metres depth. Slightly resistive material of 3000 to 10.000 Ωm, shown in blue colour in the profile, may indicate material such as fractured and water saturated bedrock (clay filled fractures commonly show resistivity response lower than 1000 Ωm). 10.000 to 35.000 Ωm, shown in green colours in the profile, indicate moderately resistive material, for example fractured and unsaturated bedrock or less fractured but water saturated bedrock. Highly resistive material, 35 000 to 150 000 Ωm indicated with orange to red colours in the profile, may consist of "unfractured" bedrock and dry, unconsolidated material.

4. STRUCTURAL SURFACE MAPPING

The rockslide reveals gneissic bedrock that is folded. There are significant variations in the orientation of the foliation, from very steep and E-W striking in the upper part, near the back scarp, to E-W striking and sub-horizontal in the lower parts. This variation in foliation occurs over a few tens of meters. In the boreholes the average dip of the foliation is 31.7°, steepening slightly from top to bottom of the slope (27° to 34°) (Kveldsvik et al., 2006).

The localities are located where bedrock is exposed, which leave large areas that are covered with vegetation or scree material unmapped (Figure 3). Vertical profiles are collected along the western boundary, where a crevasse is formed by a 20 to 40 meter high cliff.

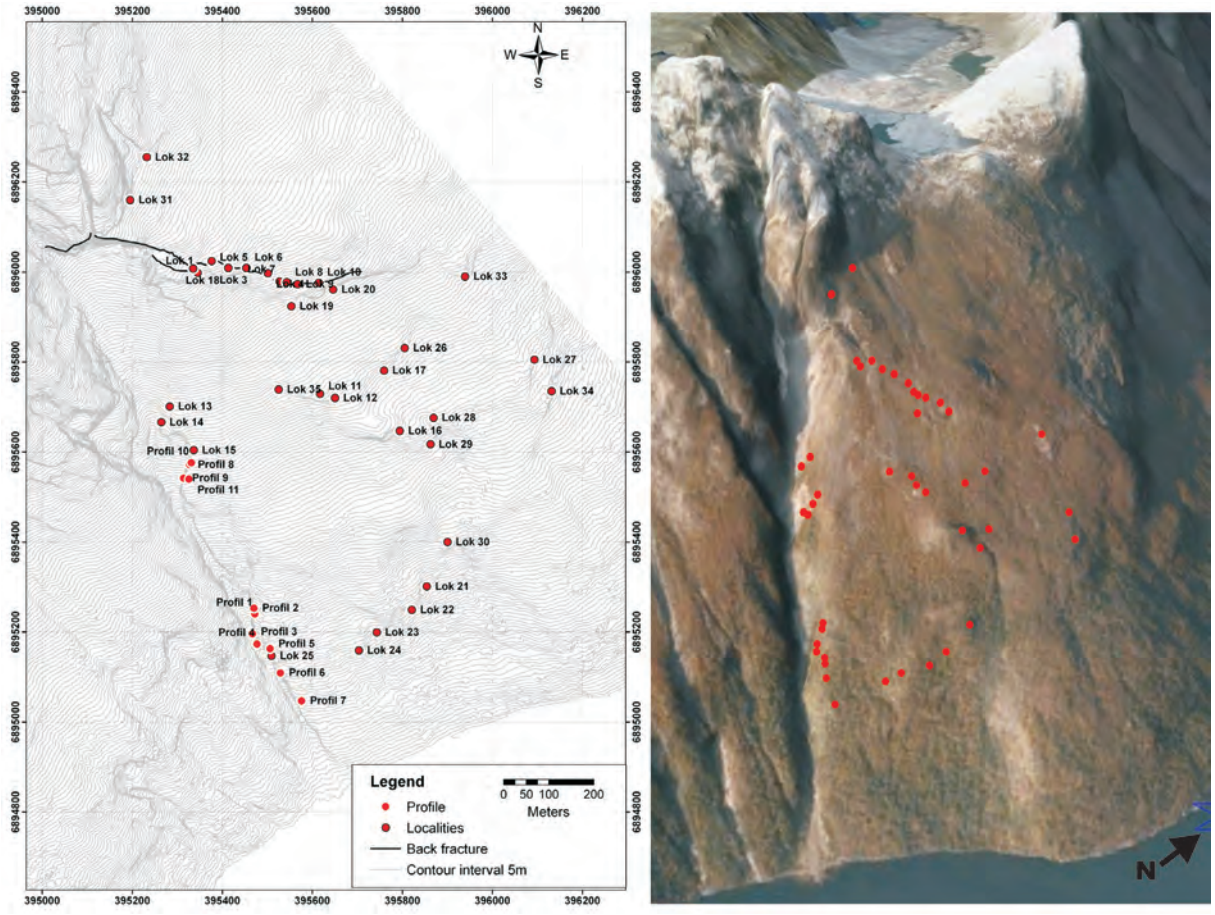

Figure 3: Localities and vertical profiles for structural surface mapping.

Structural bedrock mapping on exposures leaves a large part unmapped due to cover of vegetation and/or scree. Three distinct fracture sets are mapped within the rockslide; steeply dipping fractures with approximately N-S strike and E-W strike, and a third fracture set parallel to the foliation. The dominance and intensity of the different fracture sets vary between localities. The N-S fracture set is present at all localities; its strike varies from NNW to NNE-NE. In contrast, the E-W oriented fractures are not present at all localities, but when present, are prominent. An example is the back scarp, which partly follows E-W fracture(s). The trends of these steeply dipping fractures follow the main trends of lineaments in the region (Gabrielsen et al., 2002, Henderson et al., 2006), of which the most pronounced lineaments coincide with major fjords. Chronological data of these structures have not been assessed.

Both outcrop and drill core studies indicate an increase in fracture frequency in and near biotite rich layers of the gneiss, and with the lowest fracture frequency in the fairly homogenous granitic gneiss (Ganerød et al., 2007). The fracture frequency in outcrops varies from 2 to 8 fractures per metre (f/m) in scan lines parallel to the foliation (see section 3.1 for scan line description). Perpendicular to the foliation, foliation-parallel fracture, values as high as 23 f/m can be found. However, common values are in the ranges of 8 to 12 f/m. In the drill cores, the fracture frequency varies significantly, from 1 f/m in undisturbed rock to 50 f/m. The latter case is associated with fault rocks, such as breccias and gouge, which appears in

discrete zones. In general it is difficult to distinguish between shear and extension fractures due to the lack of markers. However, when there is evidence of opening perpendicular to the fracture surface, the structures are called extension fractures. Table 1 summarizes the fracture frequency from different zones of the area. Detailed analyses of these data are given in the following sub-sections.

Table 1: Fracture frequency (m-1), continuity of fractures sets, and block size of the different zones of the rockslide area. The value of each zone is an average based on 3 scan lines, perpendicular to and parallel to foliation, for each locality studied within that zone. From Ganerød et al. (2008).

Fracture frequency (m-1)	Back-ground data	Back Scarp Zone	Western Boundary Zone	Eastern Boundary Zone	Internal Zones	Toe Zone
Non-foliation parallel fractures	2	2	2	3	8	4
Foliation-parallel fractures	9	5	7	13	17	11
Block size						
(cm)	10 - 50	20 - 50	15 - 50	~10 - 30	5 - 20	10 - 25
Continuity of fracture sets (along strike, m)						
Foliation parallel fractures	5 - 10	~10	6 - 10	10	6 - 10	10 - 20
N-S fractures	2 - 5	0 - 2	2 - 10	2	~5	~2
E-W fractures	(1 - 2)	2 - 5	0,2 - 2		1 - 2	~1
NW-SE fractures			0,5 - 1			

4.1 Background data

The background data are based on five localities outside the rockslide area (Figure 4 and Figure 5, for localities 27, 31, 32, 33 and 34 on map Figure 3). Outside the rockslide, the fracture frequency is generally around 5 f/m. The highest fracture frequency occur perpendicular to the foliation, reaching 9 f/m, while the lowest fracture frequency is parallel to the foliation, with 2 f/m (Table 1, Figure 2). Fracture continuity of the different fracture sets has been estimated and varies within the different zones of the rockslide. For fractures outside the rockslide, the continuity parallel to foliation is 5 to 10 meters, and for N-S trending fractures, 2 to 5 meters. E-W trending fractures, while infrequent, are 1-2 meters long (Table 1).

Two localities north of the back scarp (31, 32 on map Figure 4) show that the foliation is dipping 30° to 40° towards SE, and N-S and E-W trending fractures are also present (Figure 4).

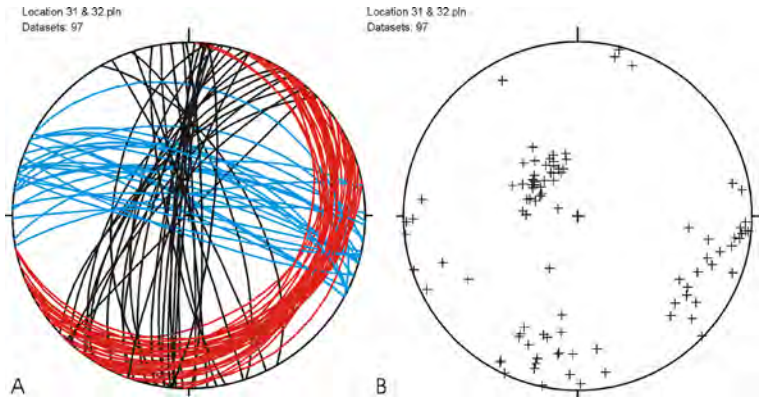

Figure 4: Stereographic projection of fracture orientation from locality 31 and 32, north of the back scarp zone. Dataset n=97. Red = foliation parallel fractures, black = ~N-S striking fractures and blue = ~E-W striking fractures.

Three localities east of the rockslide area (27, 33 and 34 on map Figure 3) show that the foliation is dipping 20° to 30° to S, and E-W and N-S trending fractures are present but not dominating (Figure 5).

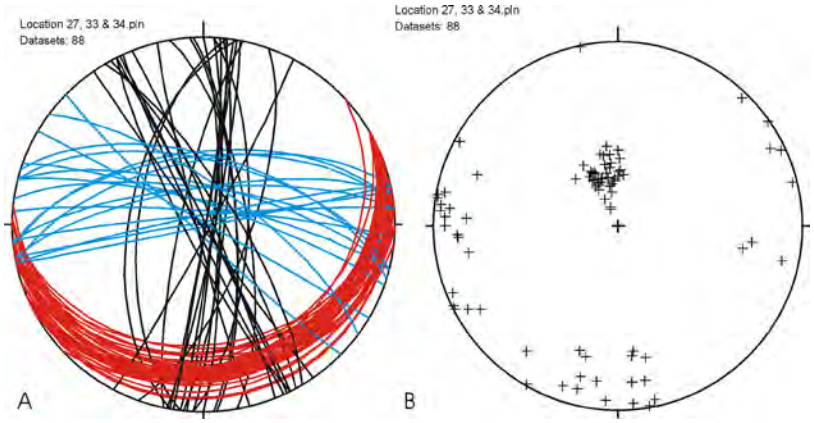

Figure 5: Stereographic projection of fracture orientation from locality 27, 33 and 34, east of the eastern boundary zone. Dataset n=88. Red = foliation parallel fractures, black = ~N-S striking fractures and blue = ~E-W striking fractures.

4.2 Back Scarp Zone

The back scarp zone is approximately 800 meters long (Figure 1). In the west, the first 200 meters is a cliff face that has seen one or more rockslides. Thereafter follows a 20-30 meter deep and 10-50 meter wide graben that shows ongoing extension. The remaining 500-600 meters is an overall open fracture. The extension along the back scarp decreases from the west to the east. The back fracture has a scissor shape, where the maximum width of 20-30 meters is found on the western side, while the width decreases towards the east, where the maximum width is 0.5-1 meter. The depth of the extensional back fracture is difficult to estimate, since the fracture is partially filled with scree, sediments and ice. The estimated depth in the western part is 60 meters, and likely decreases to the east. The back fracture shows both vertical and horizontal separation with a general extension in the N-S direction, dipping directly down-slope (Figure 6).

A striking feature of the back scarp zone is the variability in orientation of bedrock foliation. North of this zone the foliation is nearly slope parallel (Figure 6). In general, the back fracture is steep to sub vertical (Figure 6), but changes along strike as the foliation is folded (Figure 7). The folds in the back scarp zone are on meter to decimeter scale, are close to tight and normally symmetrical and have short wavelengths. The axial surfaces are sub-horizontal, and the mean vector for the fold axis is 27 degrees towards ESE. This is a regional trend which is also mapped by Henderson et al. (2006). This folding makes the foliation change from sub-vertical to sub-horizontal over short distances as shown in Figure 6 and Figure 7. Where the orientation of the foliation is favourable for extensional fracturing (i.e. when striking ~E-W and dips sub-vertical or down slope), the back fracture follows the foliation (Figure 6a and c). In contrast, where the foliation is not favourable for reactivation (i.e. when striking ~N-S and dips sub-horizontal), the back fracture reactivates pre-existing fracture sets that commonly have an E-W strike, and is steeply dipping. Locally, the back scarp zone splits into segments that form relay structures. Most relays are hard linked in that connecting fractures are cutting across the foliation between segments (Figure 6a and b). In the vicinity of the back scarp, extension fractures sub-parallel to the back scarp are common, showing a separation of 10 to 12 cm. Riemer et al. (1988) demonstrate that extension preferentially localised along the fold axis, as seen in the back scarp zone at Åknes.

In the back scarp zone all three fracture sets mentioned above are present. However, there is a dominance of N-S oriented fractures. The fracture frequency of the back scarp zone in general is low (Table 1). The length of fractures parallel to foliation is about 10 meters. In contrast, N-S trending fractures are shorter (<2 m), as are the E-W trending fractures (2-5 m, Table 1). The combination of long and short connecting fractures and low fracture frequency gives the back scarp zone the largest block size of the site.

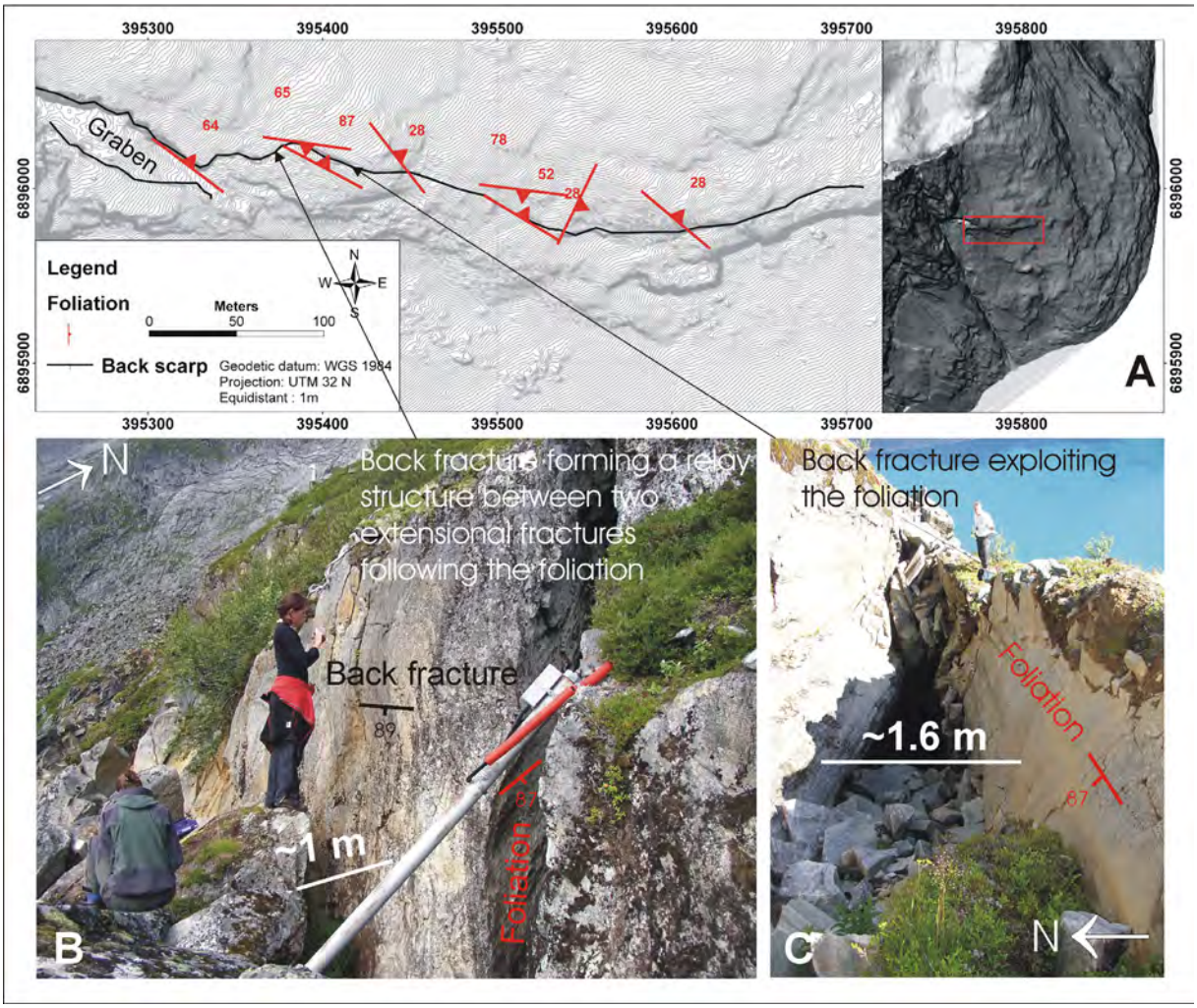

Figure 6: The foliation of the bedrock controls the development of the back scarp. Where the orientation of the foliation is favourable for extensional fracturing (i.e. when sub-vertical or dipping down slope), the back fracture follows the foliation. In contrast, where the foliation is not favourable for reactivation, the back fracture uses pre-existing fracture sets that commonly have an E-W strike, and is steeply dipping. Locally, the back scarp zone splits into segments that form relay structures (b). a) Map showing the back scarp zone and the foliation along this zone experiencing extension. b) Example of site where the foliation is not favourable and the back (extensional) fracture follows a relay structure between two larger extensional fractures, the latter following the foliation. c) Example of back fracture that is controlled by the foliation, which is sub-vertical and undulating due to mesoscopic folding. Both localities are monitored by extensometers, recording the horizontal and vertical movements along the back fracture. From Ganerød et al. (2008).

Seven localities are located along the back scarp (see map on Figure 3), which show an alternation in the foliation over a (relative) short distance (Figure 7) due to pre-existing folding.

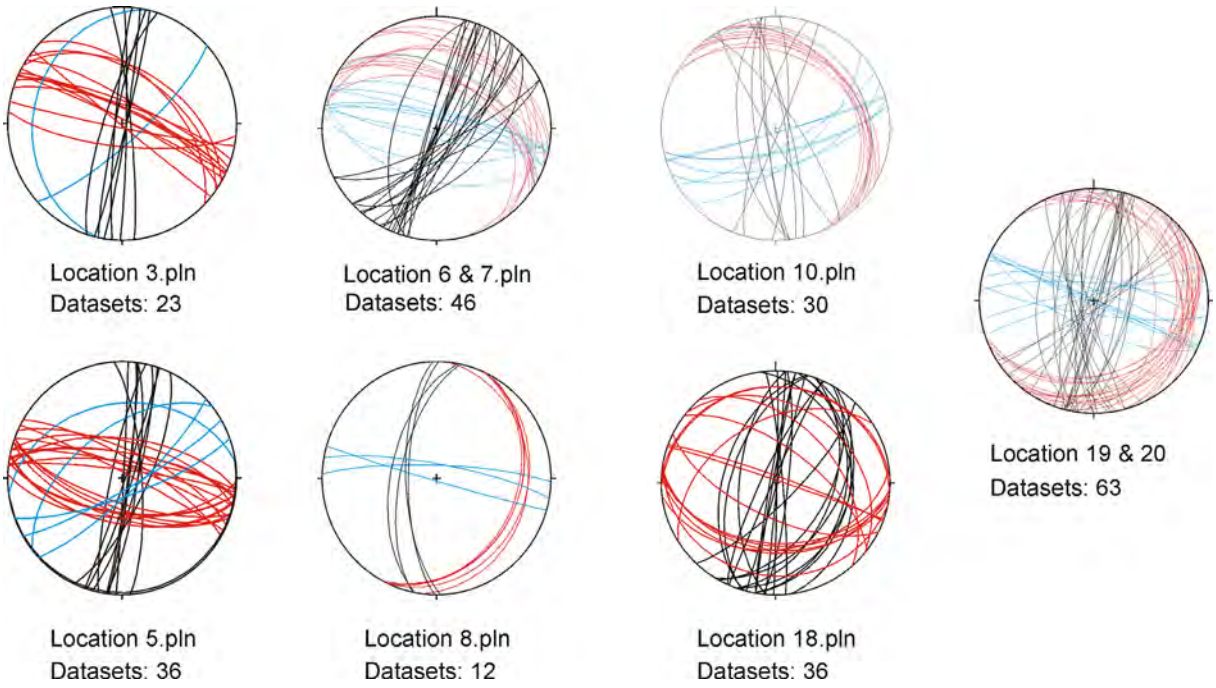

Figure 7: Stereographic projection of fracture orientation from locality 1 to 10 and 18 to 20 along the back scarp zone. Dataset n= 246. Red = foliation parallel fractures, black = ~N-S striking fractures and blue = ~E-W striking fractures. Overview of the localities are on map Figure 3.

4.3 Western Boundary Zone

The western boundary zone is the structural limitation of the rockslide to the west (Figure 1) and is defined by a steeply dipping, NNW-SSE striking, regional strike slip fault. This fault forms a crevasse that is prone to snow and rock falls. The crevasse has cliff sides that are 10 to 40 meters in height (Figure 1). The boundary fault has an extent that exceeds the rockslide area; it can be traced as a lineament for several km. This pre-existing structure is old as indicated by epidote-bearing, probably dating back to the Devonian (Osmundsen and Andersen, 2001, Braathen, 1999, Andersen et al., 1997).

In the western boundary zone, the fracture frequency is generally low (Table 1). Continuity of fracture sets reveals similarities to the back scarp, with lengths of 6 to 10 meter for foliation-parallel fractures, 2 to 10 meters for N-S trending fractures, and 0.2 to 2 meters for E-W trending fractures (Table 1). In addition, there is a NW-SE trending fracture set with 0.5 to 1 meter length (Figure 8). Within the western boundary zone, N-S oriented, steeply dipping fractures dominate (Figure 8). This fracture set is sub-parallel to the strike of the regional fault, which is defined by a zone of heavily fractured rock. In the upper part of this zone, there are several extensional fractures (Figure 9a). Some of these fractures follow the E-W and N-S fracture patterns. Extensional separation along these fractures varies from 10 to 50 cm. Three rockslide events have been recorded along the western boundary zone (Kveldsvik et al., 2006,

2007). All three appear to have occurred as planar failures, with fractures parallel to foliation acting as the basal sliding shear surfaces and N-S and E-W oriented fractures acting as tensional surfaces.

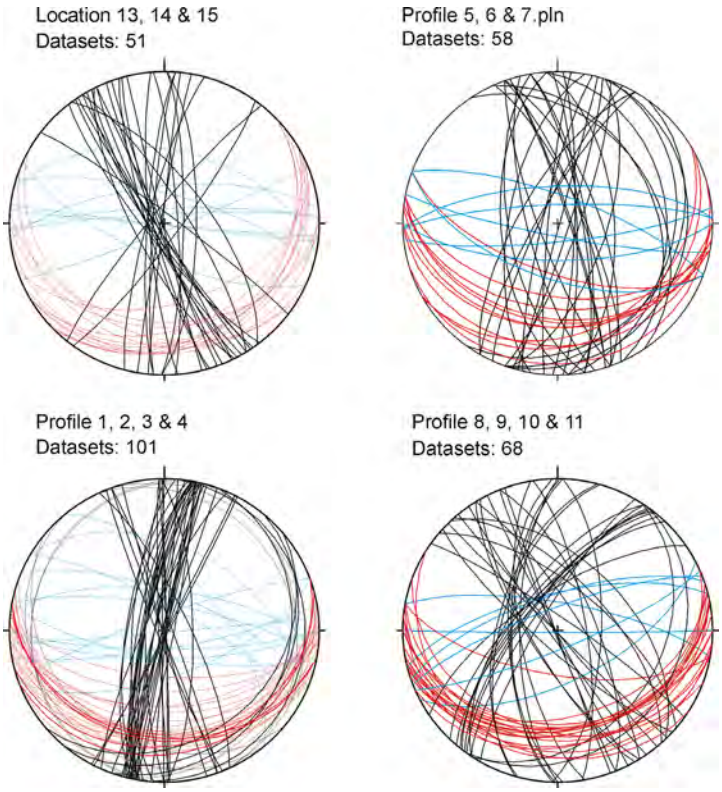

Figure 8: Stereographic projection of fracture orientation from locality 13, 14 and 15, and profiles 1 to 11, along the western boundary zone. Dataset n=278. Red = foliation parallel fractures, black = ~N-S striking fractures and blue = ~E-W striking fractures. Localities are on map Figure 3.

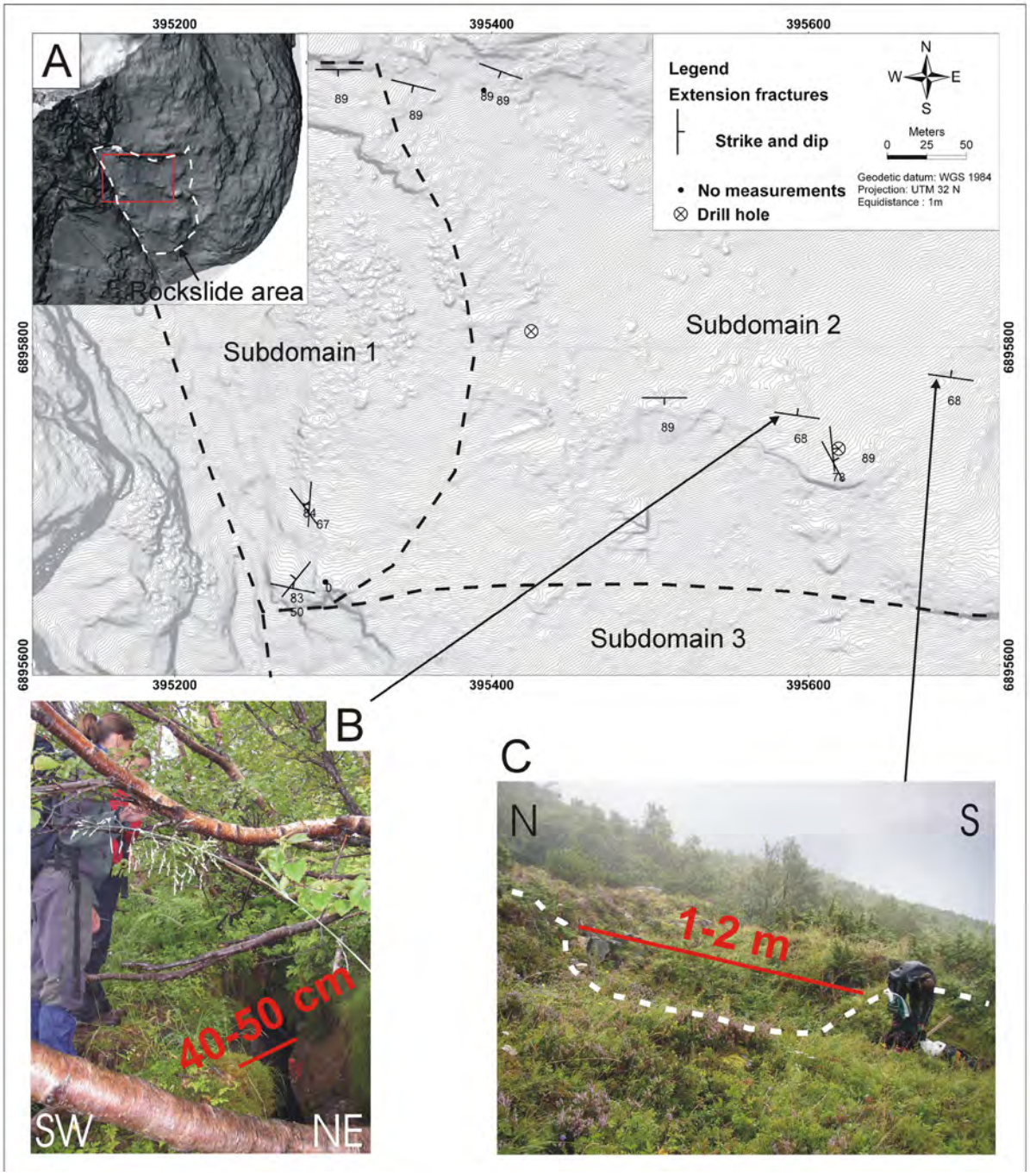

Figure 9: A) Extensional fractures located in the Åknes slope. In sub-domain 1 are pre-existing fractures oriented c. N-S and c. E-W reactivated by extension, with separation up to 50 cm. In sub-domain 2 are steep extension fractures that are slope parallel observed as shown by example B) and C) These extension fractures are oriented perpendicular to the movement direction (c. E-W trending and 60-90° dip to N-NNE), and are fractures caused by the movement of the rockslide. From Ganerød et al. (2008).

4.4 Eastern boundary zone

The eastern boundary zone represents the eastern structural limitation of the rockslide area and is defined by a gently NW dipping, NNE-SSW trending fault. This structure is not well exposed in the topography (Figure 1), possibly because it is shallow dipping and leaves no print in the topography. The fault zone is characterized by heavily fractured rock sub-parallel

to the well defined fault plane (089/48). No fault rock has been found along the fault zone, which does not rule out its existence.

The fracture frequency is higher perpendicular to the foliation (7 to 21 f/m), than parallel to the foliation (1 to 5 f/m) (Table 1). Fractures parallel to foliation are the longest, commonly in the range of 10 m, whereas N-S trending fractures reach 2 m (Table 1). E-W oriented fractures are absent (Figure 10). The foliation is in general dipping 44° to the south, which is steeper than the general trend of the foliation in the rockslide (Figure 10).

Figure 10: Stereographic projection of fracture orientation from locality 28 and 29, along the eastern boundary zone. Dataset n=63. Red = foliation parallel fractures and black = ~N-S striking fractures. Localities on map Figure 3.

4.5 Central zone

The central zone part of the rockslide area (Figure 1b), within the boundaries described above and below, reveals a sub horizontal to gently folded foliation that dips moderately towards the fjord. Folding causes an undulating geometry of the foliation. Locally, the foliation reveals more intense folds causing significant variation in the orientation. In areas where the bedrock is more intensely folded, there are hilltops and scarps suggesting that these sites are more resistant to denudation. However, the general attitude of the foliation is gently dipping towards the south (Figure 11). A foliation-parallel sliding surface in biotite rich to biotite-schist layers is mapable in outcrops of the central zone (Figure 1). This shear zone is heavily fractured with a width of 20 cm, similar to that described below and illustrated in Figure 12. Gouge can be observed as pockets along fractures, however most fractures have a rock-on-rock contact. This sliding surface forms the lower limit of sub domain 2.

The fracture frequency of the central zone is the highest recorded in the rockslide area, with the highest frequency perpendicular to the foliation (average of 17 f/m, Table 1). Parallel to the foliation, the fracture frequency is 8 f/m. The length of the fracture sets is comparable to the other zones (Table 1). The high fracture frequency in combination with fracture length gives the smallest block size (Table 1), consistent with the observations that the central zone is heavily fractured and blocky on the surface.

A striking feature in sub domain 2 is the occurrence of large extensional fractures striking approximately E-W, perpendicular to the direction of movement of the rockslide area (Figure 10). These extensional fractures have an irregular shape and have a dip of 60° to 90° in a northerly direction. The separation on these fractures is slope parallel, and varies from 40 cm to 2 m (Figure 10). Extensional movement can also be seen on N-S striking fractures, with separations of 10-30 cm, which are mapped throughout sub domain 1 and 2. The latter described fractures are probably rather frequent, but abundant coverage of scree and vegetation makes this a qualitative assessment. All fracture orientations are represented within the central zone (Figure 11). However, the foliation is dipping gently towards S, and is dominating in some areas.

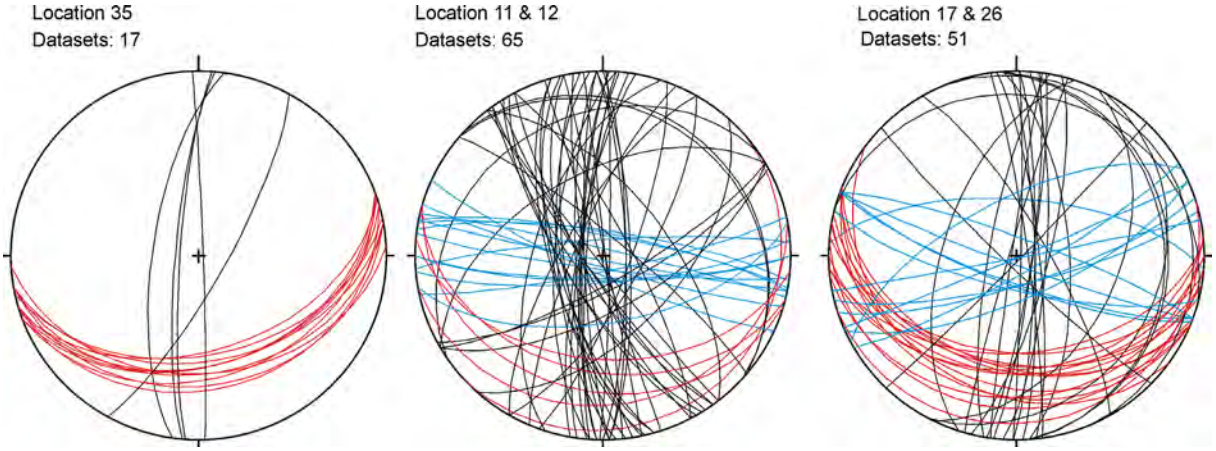

Figure 11: Stereographic projection of fracture orientation from locality 11, 12, 17, 26 and 35, in the central zone. Dataset n= 133. Red = foliation parallel fractures, black = ~N-S striking fractures and blue = ~E-W striking fractures. Localities are on map Figure 3

4.6 Toe zone

The toe zone is defined by a major sliding plane that daylights the surface (Figure 12). When observed, this sliding surface is near-parallel but shallower dipping than the topographic slope, with an orientation differing from 066/20 to 093/32. In the hanging wall, rocks are transported both upward and down-slope forming rock overhangs, at places developed into narrow, shallow caves. In these overhangs, slabs of rock have broken off along the foliation, emphasizing the position of the sliding surface (Figure 12a). The sliding surface is defined by fault rock along biotite rich layers of the bedrock, as shown in Figure 12. Locally, the sliding surface is made up of a narrow (<20 cm) heavily fractured zone. Along the long, nearly continuous exposures of the sliding surface, the fault rock interval is up to 2 cm thick (Figure 12b). The gouge layers form along-strike, metre-long lenses and/or continuous membranes of variable thickness, commonly in the range of some millimetres to a few centimetres. They are also seen in a network of shear fractures that are filled with gouge (Figure 12c). The gouge is fine grained and is light grey to dark grey. It contains clay size minerals with some (10-20 %) rock fragments. Gouge mineralogy derived from XRD-analysis includes micas, quartz and plagioclase, with micas spanning from smectite, chlorite, and kaolinite to serpentine. Where the sliding surface is defined by a heavily fractured zone, parts of the sliding surface are

characterized by rock-on-rock contact. Groundwater springs are common along the sliding surface (Figure 12), where both seepage and discrete outlets form.

The fracture frequency in the toe zone is in general 11 f/m for foliation parallel fractures and 4 f/m for non-foliation parallel fractures (Table 1), with the foliation-parallel fracture set dominating (Figure 12 and Figure 13). The length of the foliation-parallel fractures is 10-20 metres, whereas the N-S trending fractures are about 2 metres and the E-W trending fractures approximately 1 metre (Table 1).

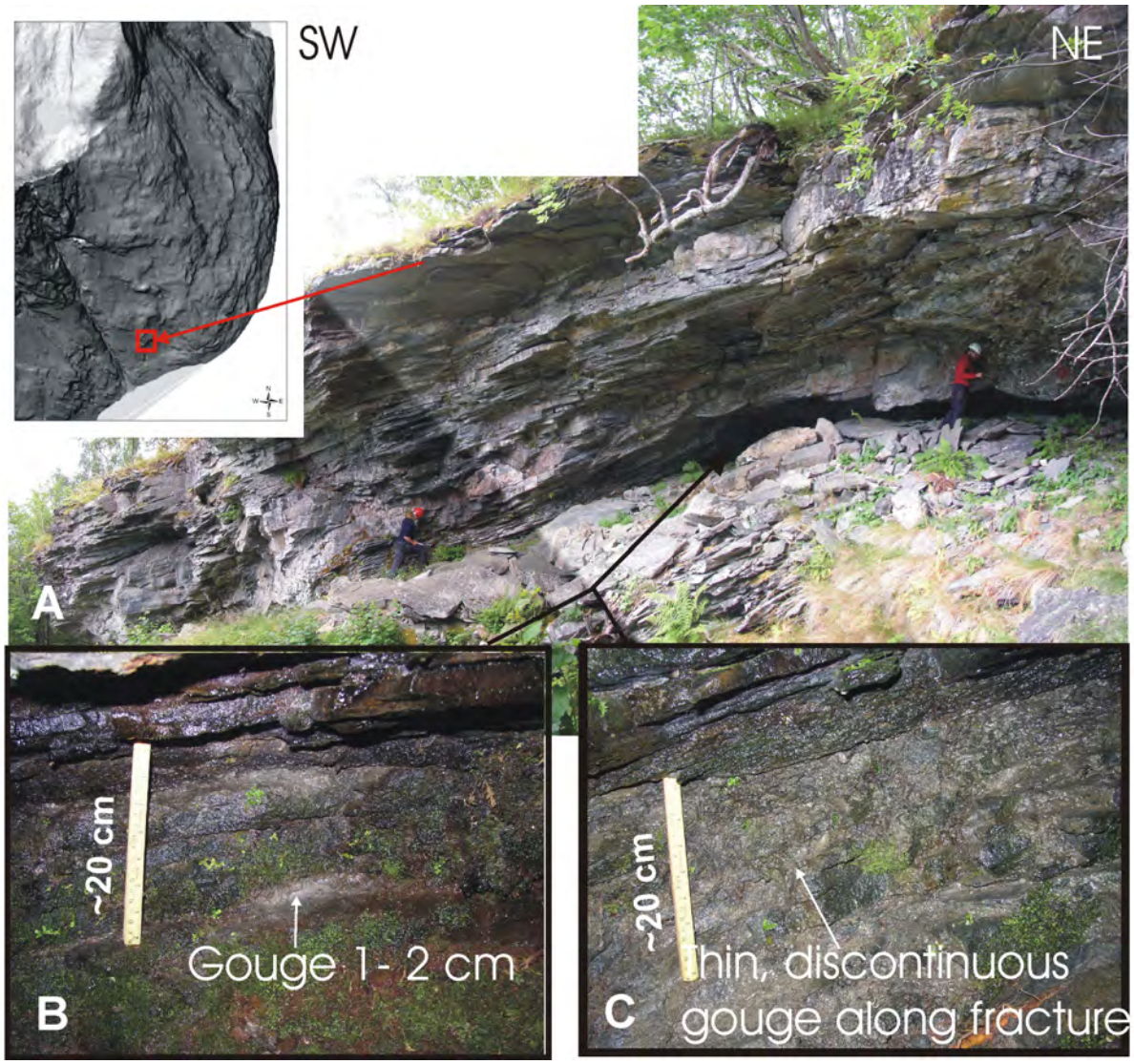

Figure 12: a) Sliding surface of the toe zone where the basal shear plane daylights the rock slope surface. Due to upward and forward separation, the transported block is pushed on top of the vegetated slope, causing the formation of a rock overhang that partly has caved in. b) Fault gouge is located as a thin layer (1-2 cm) with undulating thickness along the shear surface. (c) Example of a network of thin gouge layers that fill fractures within the intensely deformed zone of the sliding surface. This sliding surface is exposed for at least 50 metres along strike, and the thickness of the gouge rich zone is approximately 20 cm on average along the exposure. The moss growing on the fractured zone indicates water seepage. From Ganerød et al. (2008).

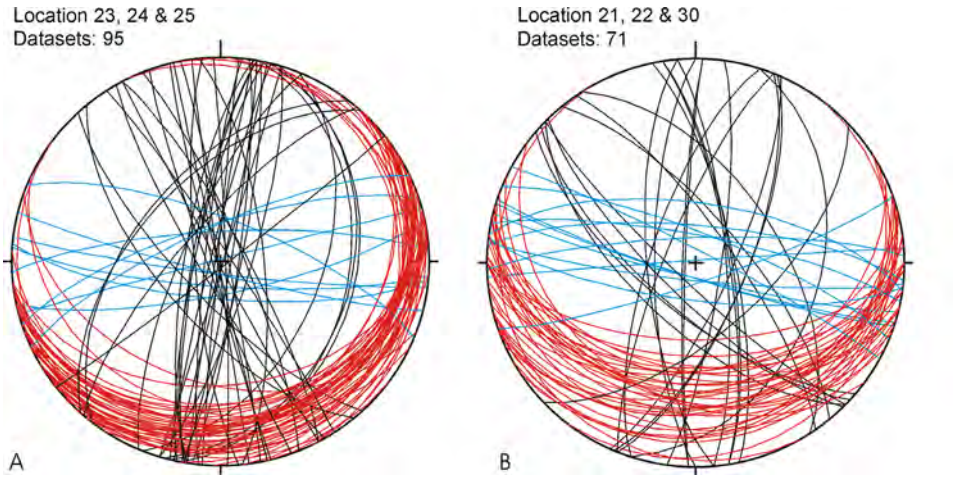

Figure 13: Stereographic projection of fracture orientation from locality 21 to 25 and 30, along the toe zone. Dataset n= 95 and 71. Red = foliation parallel fractures, black = ~N-S striking fractures and blue = ~E-W striking fractures. Localities on map Figure 3.

5. Subsurface mapping

A total of seven boreholes were drilled and cored at three sites in the rockslide area. Three holes are vertical to 150 metres depth; one is inclined by 60 degrees and goes down 150 metres, while the remaining three are vertical and 200 metres deep. All cores have been logged (Ganerød et al., 2007). The drill hole presented here is from the lowest drilling site that goes down to 150 metres depth (Figure 14).

5.1 Ground Penetrating Radar (GPR)

The profile shown in Figure 14b is a 250 m long segment of a profile with a total length of 1150 metres. Close to the surface, the reflectors of the GPR profile are parallel to the slope with a thickness of 1 to 3 metres. This first layer is interpreted to be scree material or other debris (Figure 14b). Reflectors at depth that are sub-parallel to the surface are interpreted to reflect the foliation-parallel fractures in the bedrock (Figure 14b). Two of the interpreted reflectors (marked in red, Figure 14b) daylight the surface in the same area as mapable features of the seismic and 2D resistivity profiles, indicating that multi-property layers are daylighting (Figure 14). This is interpreted to be a sliding surface. Due to the limited depth penetration, GPR cannot give any information of the extent or depth of the sliding surface. However, the method gives detailed information of the shallower subsurface. The second layer, about 25 metres thick, is interpreted to consist of heavily fractured and drained bedrock, and is comparable to the second zone identified in the seismic and 2D resistivity profiles.

5.2 Seismic

The seismic profile can be divided into four zones or intervals. The first, near surface zone is up to 5 metres thick and has a seismic velocity of 350 m/s. This zone (indicated in yellow colour in Figure 14c) is interpreted to consist of scree material. The second zone has an approximate thickness of 30 metres in the upper part and thins down to 3-5 metres down slope; the seismic velocity is about 1900 m/s. This zone is interpreted to consist of heavily fractured rock that is unsaturated (light green colour Figure 14c). The third zone is

approximately 65 metres thick, extending down to about 100 metres depth (green colour). It has a seismic velocity of 3800-3900 m/s. This interval likely consists of water saturated, fractured bedrock (Figure 14c). The fourth and deepest zone extends below the seismic resolution, and has a seismic velocity of 5500 m/s. This indicates good rock quality and is consistent with less fractured rock that is water saturated (orange colour, Figure 14c). A schematic cross section is presented in Figure 14c to illustrate estimated thickness of the different zones.

Between 300 and 330 metres along the seismic profile, a low angle zone reaching the surface has a seismic velocity of 2500 m/s. This is a lower seismic velocity than the surrounding material at 3900 m/s, consistent with high fracturing or porous rock (fault rock). The mapable, low velocity layer has a length of 30 metres at the surface. Due to methodological weakness it is not possible to map the dip of the zone. The low velocity layer might be a rather thin zone lying as a hidden layer between the 1900 m/s (light green) and 3900 m/s (green) layers (Figure 14c).

5.3 2D resistivity

The 2D resistivity profile in Figure 14d shows zonation that is interpreted to consist of an approximately 5 metres thick layer of scree material at the top (red to orange colour). Below that is a 10-20 metre thick layer (light green colour) interpreted to be heavily fractured and drained rock. The next layer has the lowest resistivity (blue colour). This layer is about 20 metres thick and is interpreted to consist of heavily fractured rock that is water saturated. This low resistivity layer is undulating and, when followed down-slope, daylights the surface at about 1200 metres (blue colour, Figure 14d). Another segment of the low resistivity layer continues down-slope. The sliding surface is interpreted as being located at the bottom of this low resistivity layer (blue colour). Near the base of the profile is a layer with medium resistivity (green colour), interpreted to consist of less fractured and water saturated bedrock (**Figure 14**d).

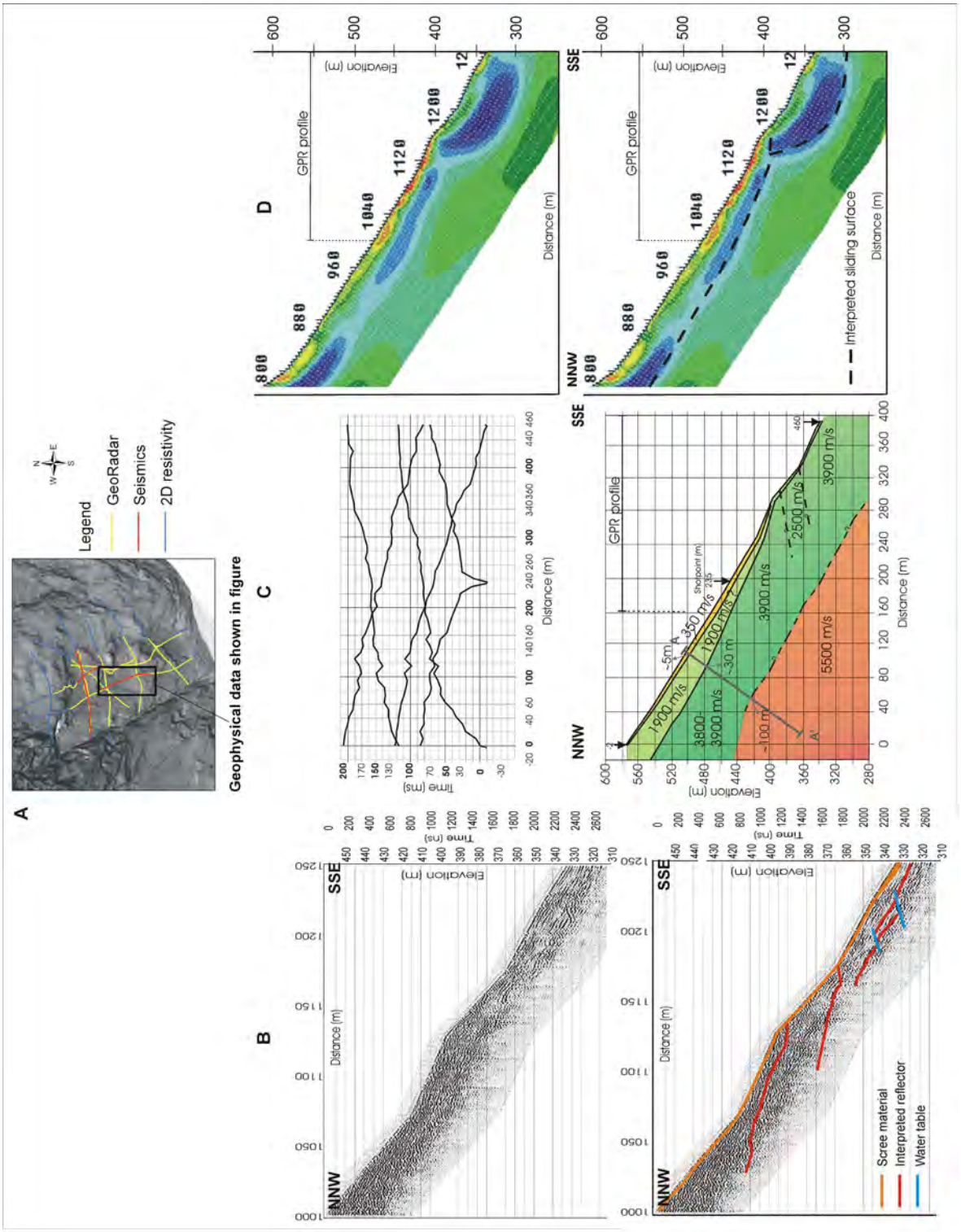

Figure 14. Geophysical data from Åknes. A) Map showing all the geophysical profiles collected in the rockslide area. The presented profiles b-d are only a selected section of a profile. Profile c and d are the same section, c. 450 m long, while b is 250 m long and its location is marked in profile d. B) GPR profile with NNW-SSE orientation and approximate 35 m depth penetration. Above, profile without interpretations, below; profile showing shallow, undulating structures, interpreted to be foliation-parallel layers that crop out at the slope surface (marked with red lines). C) Refraction seismic; above travel time (ms) vs. distance (m) for first arrival P-wave traces. Below, schematic profile showing four layers with increasing velocities with depth. A-A` is line of cross section for thickness estimates. D) 2D resistivity profile, measured with Wenner configuration, showing layers with different resistivity. Above, profile without interpretation, below; profile showing an undulating resistivity contrast, interpreted as a sliding surface at the bottom of the low resistivity (blue) layer marked with black dashed lines. The profile has the same location as the seismic line (c).

6. DISCUSSION

6.1 Geological model based on observations

Observations and interpretations of data (summarize on map in Figure 15) described above in five significant structural zones form the basis for the geological model of Åknes rockslide area, as illustrated in Figure 16. The style of deformation, with bearing on the geometry of the rockslide area, is that of an extensional fault system at the top and an imbricate thrust fan further down-slope. In other words, the rock slope failure can be divided into two; an upper part experiencing extension (Figure 1 and Figure 6), and a lower part deforming by compression (Figure 1 and Figure 12). The basal sliding surface split into four subordinate planes. They form sliding surfaces along which sub-domains are partially stacked. Two of the sliding surfaces, crop out (and bound sub-domain 2 and 4, Figure 15) and two are indicated by geophysics (and bound sub-domain 1 and 3, Figure 16). The depth to the sliding surfaces differs within the four sub domains. In an east-west cross-section, the depth to the sliding surface shows a general increase to the west and decrease to the east. Down-slope, the sliding surfaces have roughly the same depth, and cut up-section near the toe of the thrust sheet (Figure 16). The length and width of the sliding blocks are fairly similar (Figure 16).

To summarize, the structural mapping of the area shows that the foliation is undulating along and across the slope. It controls the development of the back scarp and the basal sliding surface and its subordinate thrust zones. Along the back scarp, extension perpendicular to the fold axis is common when it is favourable, giving open fractures along the sub-vertical foliation (Figure 6c). Down-slope the foliation is sub-parallel to the topographic slope, and where the foliation dips shallower than the slope, there are thrusts daylighting the surface as seen at two levels down-slope (Figure 12 and Figure 15). The rockslide area can be further divided into five structural zones based on surface characteristics, where the upper structural limitation of the rockslide is the back scarp zone with its scissor like shape (Figure 6 and Figure 15). The separation along the back scarp zone is gradual and constant on a yearly basis, with a larger movement of the western side than on the eastern. The western boundary zone is the structural western limit of the rockslide area with a prominent crevasse formed along a NNW-SSE trending strike slip fault. The eastern structural limit of the rockslide area coincides with a pre-existing large fault zone (Figure 1 and Figure 15). The central zone of the rockslide can be divided into four sub-domains separated by subordinate, low angled, sliding surfaces seen on the surface and interpreted from geophysics (Figure 15 and Figure 16). In sub-domain 2, several extensional fractures with slope-parallel separation of up to 2 meters are located (Figure 10). These structures have formed perpendicular to the displacement direction. Sub-domains 3 and 4 have less distinct features, but the occurrence of springs increases down-slope. The toe zone is the lower limit of the rockslide and is defined by a subordinate sliding surface that can be observed at the surface (Figure 12). The sliding surface is mapped as a low-angle thrust-like structure that is more or less continuous. The interpretation of the sliding surface at the toe zone is as a thrust ramp that daylight the surface, consistent with compression in the toe zone (Figure 16).

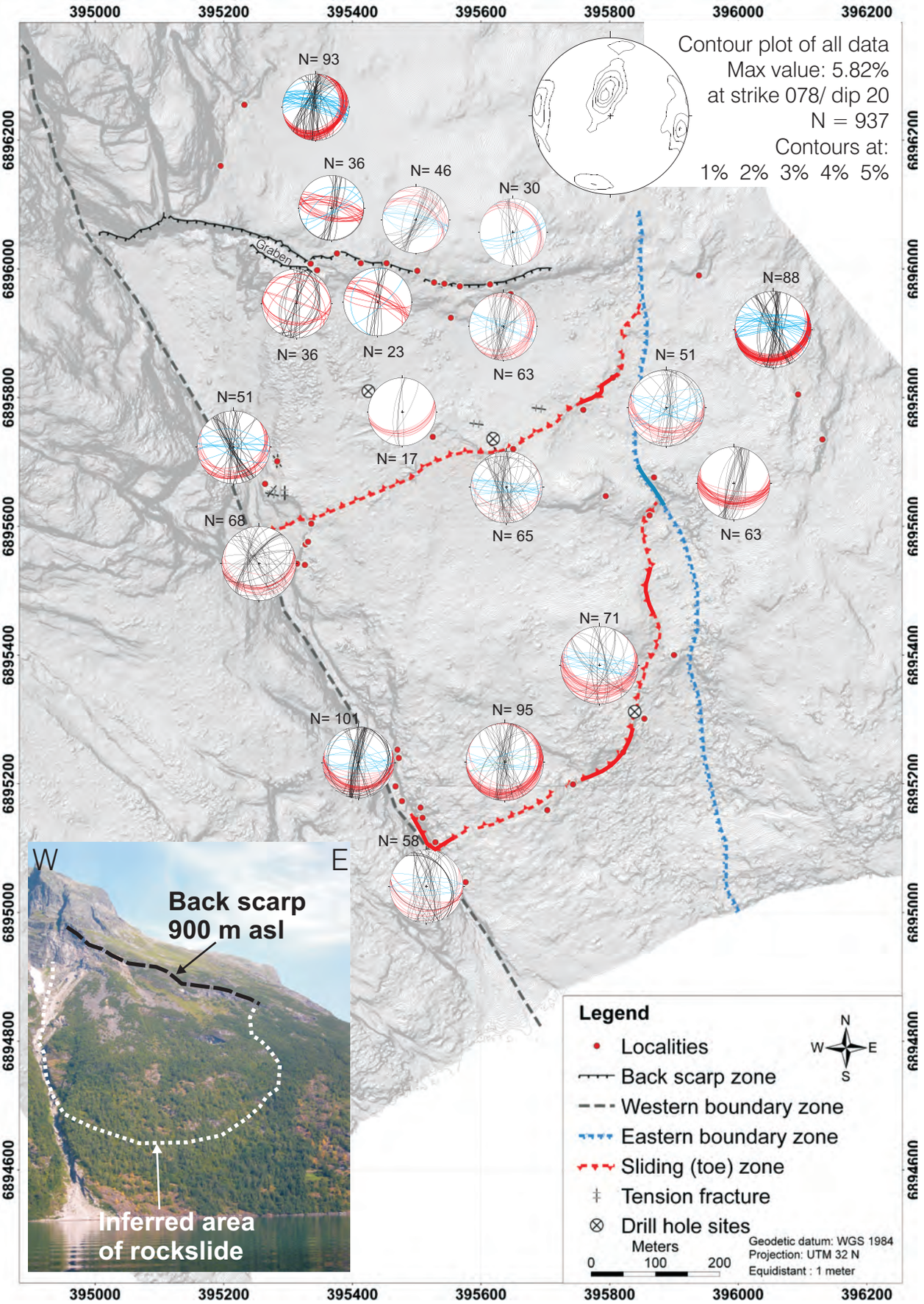

Figure 15: Relief map of the Åknes site with stereographic presentation of the fracture distribution compiled from all localities studied. The picture (lower left) outlines the inferred area involved in the rockslide (photo: M.H. Derron). The stereographic projections show great circles (lower hemisphere equal area) of fractures mapped at different localities, where c. N-S striking fractures are black, c. E-W striking fractures are blue and fractures parallel to the foliation are red. Structural symbols outline tectonic boundaries along the margin and inside the rockslide area. The western boundary zone is a NNW-SSE striking and sub-vertical, strike-slip fault, whereas the eastern boundary zone is a pre-existing fault with shallow dip to the west. The upper boundary is seen as a pronounced back scarp. Low angle sliding surfaces daylights at two levels in the slope, marked with a red hatched line (sub-domain 2 and 4), while two sliding surfaces are mapped by geophysics, marked with red dashed lines (sub-domain 1 and 3). The foliation is folded and changes within the rockslide, strike 092/ dip 44 (RHR) at the western boundary zone, 080/ in sub-domains 2, and the toe zone differs from 066/20 to 093/32 (n=137). From Ganerød et al. (2008).

An interpretation of the eight 2D resistivity profiles in a tied grid, supplemented with drill hole data, GPR and seismic profiles, formed the basis for the mapping of the subsurface with respect to the sliding surfaces (Figure 14) and, furthermore, the geological model of the rockslide area (Figure 15 and Figure 16). The structures interpreted in the subsurface from geophysical data coincide well with structures mapped on the surface. In addition, the geophysical data indicate the position of the sliding surfaces in the subsurface (Figure 14). The two outcropping sliding planes, between sub domains 1 and 2 and between sub domain 4 and the toe zone (Figure 15), are also well covered with geophysical data (Rønning et al., 2006), indicating the lateral extent of the sliding surfaces where they are covered by vegetation and scree (Figure 15 and Figure 16). Furthermore, this forms the basis for the extrapolations of the sliding surfaces where they are not exposed (Figure 15 and Figure 16). The geophysical data indicate two additional sliding surfaces (Rønning et al., 2006, Figure 16), with similar signatures to the two observed at the surface. These divide the central zone into four sub-domains as indicated in Figure 16. All the sliding surfaces interpreted by 2D electric resistivity have an undulating character, and daylight the surface along the slope. They are shown as low resistivity zones and the sliding surfaces are interpreted to be located at the bottom of these zones (Figure 14). The geophysical data also supports the location of the larger structures forming the western boundary, as a sub-vertical structure, and eastern boundary as a gentle, westward dipping structure (Rønning et al., 2006).

All observations of the basal sliding surface indicate that it is undulating. Undulations imaged by geophysics can be caused by three scenarios; 1) growth of the sliding surface as segments, where the undulating composite surface is made up of several connected slip planes and where undulations reflect broken fault segments. 2) heterogeneous biotite schist layer extent and distribution, where layers of biotite schist are linked by fractures, and 3) reactivated folded foliation. Due to the evidence that the foliation is folded, as shown in Figure 15, and the fact that the foliation controls the development of the basal sliding surface with its subordinate low angle thrust zones (Figure 12), the reactivated, folded foliation model is plausible, either as the main controlling factor, or in combination with the other two.

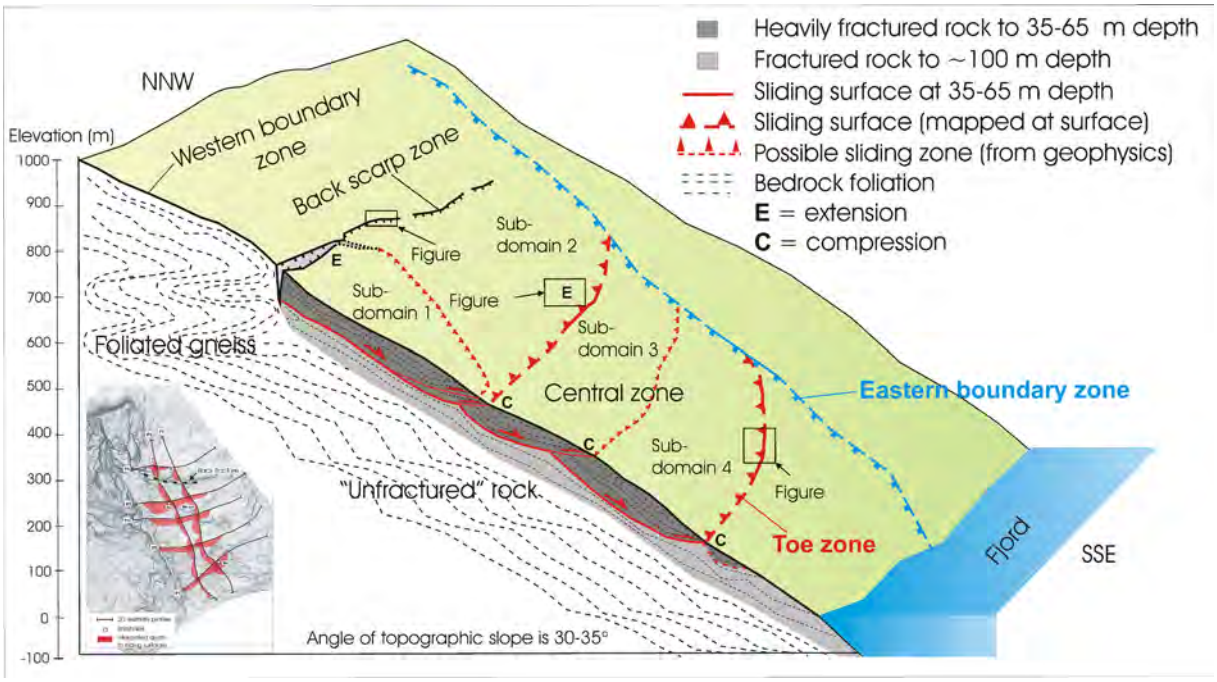

Figure 16: Geological model of the Åknes rockslide. The block diagram summarizes field observations and geophysical data (Rønning et al., 2006). Interpretation of structural data correlated well with structural interpretation from the 2D resistivity profiles (left, bottom corner), suggesting an undulating basal sliding surface with subordinate sliding surfaces that crop out at several levels of the slope. The rockslide can be divided into four sub-domains with different structural characteristics, where two of the marked sliding surfaces are mapped at the surface and two sliding surfaces are interpreted from geophysical data (Figure 14d, Rønning et al., 2006). The depth to the basal sliding surface varies, but in general increases towards the west. Structural constraints of the rockslide borders to the east and west are pre-existing large faults. The top is delineated by an extensional back scarp. The toe zone forms the lower limit of the rockslide. The foliation is folded, especially in the back scarp zone, but also shows gentle variations down-slope and across-slope, as indicated in the figure by black dashed lines (Ganerød et al., 2008).

6.2 Geological model in light of other studies

Considering Varnes` (1978) classification of landslide types, Åknes rockslide does not simply fit into one category but forms a complex landslide, which is a combination of two or more principal types of movement. Creep is considered to be continuous in the Åknes rockslide, contributing to the general deformation of the bedrock and displacement of the rockslide. In the upper part of the Åknes rockslide, sub-domain 1 and 2, indications of rotational slide movement is observed in the combination of vertical and horizontal movement of the back scarp as well as backward tilting of blocks (Figure 6 and Figure 16). Translational slide movement is observes along the western flank of the rockslide, especially in sub-domain 1, where abundant extensional fractures (tension cracks) in a range of sizes are observed, both with ~N-S and ~E-W strike (Figure 10). However, the toe zone and the eastern flank, primarily sub-domain 3 and 4, of the Åknes rockslide does not fit within Varnes` (1978) classification. This is hereby argued due to control of pre-existing structures such as the fault forming the western boundary zone and the ductile fabric of the bedrock, i.e. the foliation controlling the basal sliding surface with its subordinate thrusts that daylights at several levels, but is most prominent in the toe zone (Figure 12, Figure 15 and Figure 16). Another argument for the distinctly different appearance is that the Åknes rockslide has not evolved

far enough to display the common structures occurring in “the zone of accumulation” according to Varnes` (1978) classification. Anyhow, the basal sliding zone with its subordinate sliding surfaces observed at Åknes rockslide form thrusts, giving compression, and display as an imbricated thrust fan (Figure 15).

Braathen et al. (2004) define Åknes rockslide as a *rockslide area*, given that the rockslide area has a relative low gradient (<45°), weakness zones sub-parallel to the surface, and movement in the lower parts leading to failures in the upper part of the slope. These weakness zones are, for example, foliation and/or layering or pre-existing fractures oriented sub-parallel to the slope. Results from this study support the view that Åknes is a rockslide area, but has a more complex structure (Figure 1 and Figure 16). Braathen et al. (2004) further address the rockslide kinematics in a down-slope direction. Results from this study imply that Åknes fits with Braathen et al.`s (2004) model of the combined extension – compression scenario, predicting a high frontal friction.

Oppikofer and Jaboyedoff (2007) proposes another type of model of Åknes rockslide based on DEM (digital elevation model) and ground-based Lidar image analyses of Åknes and surrounding occurred and potential rockslides. They use the asperity-amplitude method to estimate the roughness of the foliation which gives the geometry of the basal sliding surface, and analysis of spatial distribution of steep fractures. This provides a model with primarily planar back scarps and a stepped basal sliding surface, where the rockslide is mainly translational in type. This is a model similar to that of Eberhardt et al. (2004) described as “sequential failure with internal shearing with yielding of rock bridges” or “multiple step-path failure with intact rock bridges”. The sequential failure model is similar to that proposed for the Randa rockslide (Eberhardt et al., 2004). Eberhardt et al. (2004) demonstrate that where sliding surfaces are predefined and controlled by pre-existing structures less internal rock deformation is needed to achieve failure of the rockslide. Tension cracks are commonly an indication of internal rock deformation, and with regards to Åknes rockslide both persistent pre-existing structures and tension cracks are observed, indicating a more complex deformation mechanism with possibly a combination of brittle and ductile behaviour (Eberhardt el al., 2004). This may be the essential difference between the model of Åknes rockslide presented by Oppikofer and Jaboyedoff (2007) and the one proposed in this work. The model by Oppikofer and Jaboyedoff (2007) is not considering the properties of the bedrock as strongly and showing brittle behaviour, while we propose a model where the ductile fabric highly control the geometry of the gravitationally driven brittle structures. As the undulated planes are a reactivation of the undulated foliation.

The most realistic model of Åknes rockslide is probably a combination of that proposed here and that of Oppikofer and Jaboyedoff (2007). However, the morphology of the rockslide models after failure is likely to be similar.

Giraud et al. (1990) gives examples of rockslides controlled by pre-existing structures, such as foliation, where the slope parallel foliation forms potential slip planes, which increase the potential of rockslides progressing into rock avalanches with minor changes in physical or hydrogeological conditions as trigger. These are conditions that are valid for Åknes rockslide,

and emphasises the importance of pre-exiting structures as a controlling factor. Giraud et al. (1990) also argue that rockslides with pre-existing structures controlling the slip surface are more likely exposed to translational or rotational types of movement. Another model that has been proposed is the deep-seated slope gravitational deformation model (DSGSD); a model that shows only extension (Agliardi et al., 2001, Crosta and Agliardi, 2003). An example of such DSGSD is the Ruinon rockslide (20 mill. m^3) of the Italian Alps. This deep-seated slope gravitational deformation indicates one deep, more or less continuous sliding surface, and collapse of the lower part of the slope (Agliardi et al., 2001). At Åknes there is no indication of collapse in the lower part of the slope and there is evidence of several sliding surfaces as well as a combined extension – compression regime, making this model less viable for this site. Seno and Thüring (2006) propose several different landslides models, based on case studies from the Swiss Alps, varying from rotational rockslides to rock slump, sag or deep-seated creep and retrogressive landslide. However, these examples seems to commonly be triggered by alteration in groundwater level, and by reactivation along pre-existing structures such as faults and foliation of the bedrock, even though two of the case studies have slope parallel schistosity (Seno and Thüring, 2006).

Numeric modelling tools are widely used for kinematic analyses and stability calculation of rock slope (Eberhardt et al., 2004, Stead et al., 2006), however, due to the large uncertainties in input parameters the use of numerical modelling is mainly limited to back analysis (Meric et al., 2005). Therefore, the need for geological data to constrain the models is critical, and this work is an attempt of achieving constraints on geological parameters that will be applied in numeric models (Kveldsvik et al., 2007).

6.3 Fracture distribution

Two hypotheses are entertained for the existing fracture sets mapped in the rockslide area. Firstly, they are pre-existing fractures, probably of Devonian age, which are reactivated due to movements on the basal sliding surface. Since all recorded fracture sets are present throughout the rockslide area (Figure 15), this indicates that the fractures are pre-existing. Some of the fractures are reactivated due to shear movement along the basal sliding surface, which coincides with results of Henderson et al. (2006) from regional studies in the vicinity of Åknes. In the second hypothesis, the fracture sets are caused by shear movement along the sliding surface. Slope parallel fractures or fractures that form perpendicular to the displacement direction are indications of fractures caused by movement of the rockslide. Sub-vertical extensional fractures (i.e. tension cracks), which seem to occur randomly, have a strike (~E-W) more or less perpendicular to the direction of movement (SSW) are observed in sub-domain 2 (Figure 10 and Figure 15). This phenomenon is also observed in other sites in the vicinity (Henderson et al., 2006). At Åknes both types of fractures occur, but the majority of fractures are reactivated older structures. In addition, logging of the drill cores show that the fracture frequency decreases with depth, indicating reactivation of pre-existing fractures and/or foliation rather than initialization of new fractures (Ganerød et al., 2007).

7. CONCLUSIONS

- The folded foliation controls the development of the back fracture. Where the orientation of the foliation is favourable for extensional fracturing (i.e. when sub-vertical or dipping down slope), the back fracture follows the foliation.

- The folded foliation controls the development of the basal sliding surface with its sub-ordinate sliding surfaces as low angle trusts; i.e. the sliding surface is undulating due to gentle folds in the foliation of the bedrock. The sliding surfaces are mapped where they daylight the surface, and are characterized by the occurrence of fault rocks such as gouge and breccia. In general, the depth to the sliding surfaces varies due to the undulation, generally increasing to the west and decreasing to the east, with a maximum depth of 65-70 metres.

- The rockslide area is divided into four sub-domains, confined by sub-ordinate low angle thrusts that daylight the surface. These sub-domains have different displacement patterns and rates, and have the down-slope geometry of an imbricated fan. Extension characterizes the two upper domains of the rockslide whereas compression characterizes the two lower domains.

- The rockslide area is structurally confined with the upper rockslide limit formed by the back scarp zone, whereas a pre-existing NNW-SSE strike slip fault forms the western boundary zone. The eastern boundary zone is a gentle westward dipping pre-existing fault, and the toe zone forms the lower limit, where a sliding surface daylights the surface.

Acknowledgements
Thanks go to Stranda Municipality for finance and management of the Åknes / Tafjord project, and to the International Centre of Geohazards (ICG) for project management and cooperation. Thanks to Aline Saintot for constructive comments on the manuscript.

8. REFERENCES

Agliardi, F., Crosta, G., Zanchi, A. (2001). Structural constraints on deep-seated slope deformation kinematics. Engineering Geology, 59, pp. 83-102

Andersen, T.B., Osmundsen, P.T., Berry, H.N., Torsvik, T.H., Eide, E.A. (1997). Multi-level detachments and exhumation in the Norwegian Caledonides. Abstracts with Programs - Geological Society of America 29, (6), pp. 317

Blikra, L.H., Longva, O., Braathen, A., Anda, E., Dehls, J., Stalsberg, K. (2005a). Rock-slope failure in Norwegian fjord areas: examples, spatial distribution and temporal patterns. In Evans, S.G., Scarascia Mugnozza, G., Strom, A.L. & Hermanns, R.L. (eds.): *Massive rock slope failure: new models for hazard assessment*, Kluwer, Dodrecht.

Blikra, L.H., Longva, O., Harbitz, C., Løvholt, F. (2005b). Qualification of rock-avalanche and tsunami hazard in Storfjorden, western Norway. In Senneset, K., Flaate, K. & Larsen, J.O. (eds.): *Landslide and Avalanches ICFL 2005 Norway*, Taylor & Francis Group, London.

Braathen, A., Blikra, L.H., Berg, S., Karlsen, F. (2004). Rock-slope failures of Norway; types, geometry, deformation mechanisms and stability. Norwegian Journal of Geology 84, (1), pp. 67-88

Braathen, A. (1999). Kinematics of post-Caledonian polyphase brittle faulting in the Sunnfjord region, western Norway. Tectonophysics 302, (1-2), pp. 99-121

Crosta, G.B., Agliardi, F. (2003). Failure forecast for large rock slides by surface displacement measurements. Canadian Geotechnical Journal, Vol. 40, pp. 176-191 ://cgj.nrc.ca

Dahlin, T. (1993). On the Automation of 2D Resistivity Surveying for Engineering and Environmental Application. Ph.D. thesis, Lund Technical University, Sweden

Davis, G.H., Reynolds, S.J., (1996). Structural geology of rock and regions. 2nd ed. Wiley & Sons, pp. 776

Derron, M.H., Blikra, L.H., Jaboyedoff, M. (2005). High resolution digital elevation model analysis for landslide hazard asessment (Åkerneset, Norway). In Senneset, K., Flaate, K. & Larsen, J.O. (eds.): *Landslide and avalanches ICFL 2005 Norway*, Taylor & Francis Group, London.

Eberhardt, E., Stead, D., Coggan, J.S. (2004). Numeric analysis of initiation and progressive failure in natural rock slopes – the 1991 Randa rockslide. Rock Mechanics and Mining Sciences, 41, pp. 69-87.

Elvebakk, H. (2008). Borehullslogging, Åknes, Stranda kommune. NGU-rapport 2008.030, 36 s., Norges geologiske undersøkelse

Gabrielsen, R.H., Braathen, A., Dehls, J., Roberts, D. (2002). Tectonic lineaments of Norway. Norwegian Journal of Geology, 82, pp. 153-174

Ganerød, G.V., Grøneng, G., Rønning, J.S., Dalsegg, E., Elvebakk, H., Tønnesen, J.F., Kveldsvik, V., Eiken, T., Blikra, L.H., Braathen, A. (2008). Geological model of the Åknes rockslide, western Norway, Engineering Geology, doi:10.1016/j.enggeo.2008.01.018. http://dx.doi.org/10.1016/j.enggeo.2008.01.018

Ganerød, G.V., Grøneng, G., Aardal, I.B., Kveldsvik, V. (2007). Core logging of seven boreholes from Åknes, Stranda municipality, Møre and Romsdal County. NGU report no. 2007.020, pp. 222

Giraud, A., Rochet, L. and Antoine, P. (1990). Processes of slope failure in crystallophyllian formations. Engineering Geology, 29, pp. 241-253.

Henderson, I.H.C., Saintot, A., Derron, M.H. (2006). Structural mapping of potential rockslide sites in the Storfjorden area, western Norway: the influence of bedrock geology on hazard analysis. NGU report no. 2006.052, pp. 1-82

Hermanns, R.L., Blikra, L.H., Naumann, M., Nilsen, B., Panthi, K.K., Stromeyer, D., Longva, O. (2006). Examples of multiple rock-slope collapses from Köfels (Ötz valley, Austria and western Norway. Engineering Geology, 83, pp. 94-108

Kveldsvik, V., Nilsen, B., Einstein, H.H., Nadim, F. (2007). Alternative approaches for analyses of a 100.000 m^3 rock slide based on Barton-Bandis shear strength criterion. Landslides, DOI 10.1007/s10346-007-0096-x

Kveldsvik, V., Eiken, T., Ganerød, G.V., Grøneng, G., Ragvin, N. (2006). Evaluation of movement data and ground conditions for the Åknes rock slide. The International Symposium on Stability of rock slopes, at the South African Institute of Mining and Metallurgy, April 2006, pp. 1-24.

Loke, M.H. (2001). RES"INV version 3.4. Geoelectrical Imaging 2D & 3D. Instruction manual. (10.15.2004)

Meric, O., Garambois, S., Jongmans, D., Wathelet, M., Chatelain, J.L., Vengeon, J.M. (2005). Application of geophysical methods for the investigation of the large gravitational mass movement of Séchilienne, France. Canadian Geotechnical Journal, 42, pp. 1105-1115.

Oppikofer, T., Jaboyedoff, M. (2007). Åknes/Tafjord-Project: DEM analysis of the Rundefjellet/Tårnet area, Report IGAR-TO-005, University of Lausanne, Switzerland.

Osmundsen, P.T., Andersen T.B. (2001). The middle Devonian basin of western Norway; sedimentary response to large-scale transtensional tectonics? Tectonophysics, 332, pp. 51-68

Reynolds, J.M. (1997). An Introduction to Applied and Environmental Geophysics. John Wiley & Sons, New York, pp. 796.

Riemer, U.T., Lecher, T., Nunez, I. (1988). Mechanics of deep seated mass movements in metamorphic rocks of the Ecuadorian Andes. Proceedings of the 5th International Symposium on Landslides, Lausane, 1988. Balkema, 1990.

Roth, M., Dietrich, M., Blikra, L.H., Lacomte, I. (2006). Seismic monitoring of the unstable rock slope site at Åknes, Norway. SAGEEP - Symposium on the Application of Geophysics to Engineering and Environmental Problems, Extended abstract

Rønning, J.S., Dalsegg, E., Elvebakk, H., Ganerød, G.V., Tønnesen, J.F. (2006). Geofysiske målinger Åknes og Tafjord, Stranda og Nordal kommune, Møre og Romsdal. NGU report no. 2006.002, pp. 1-66

Rønning, J.S. ; Dalsegg, E. ; Heincke, B.H. ; Tønnesen, J.Fr. (2007). Geofysiske målinger på bakken ved Åknes og ved Hegguraksla, Stranda og Nordal kommuner, Møre og Romsdal. NGU-rapport 2007.026, 60 s. Norges geologiske undersøkelse.

Seno, S., Thüring, M. (2006). Large landslides in Ticino, Southern Switzerland: Geometry and kinematics. Engineering Geology 83, pp. 109-119

Stead, D., Eberhardt, E., Coggan, J.S. (2006). Developments in the characterization of complex rock slope deformation and failure using numerical modeling techniques. Engineering Geology, 83, pp. 217-235

Tveten, E., Lutro, O., Thorsnes, T. (1998). Berggrunnskart Ålesund. 1:250000, (Ålesund, western Norway), NGU Trondheim (bedrock map)

Varnes, D.J. (1978). Slope movement types and processes. In: Schuster, R.L., Krizek, R.J. (Eds.), Landslides – Analysis and Control, U.S. National Acadamy of Science, Special Report, Vol. 176, 2, pp. 11-33.

9. APPENDIX

Table 2: Below are all localities listed with coordinates and description.

	WGS 1984, UTM zone 32				
Name	East	North	m above sea-level	Accuracy (+/- m)	Description
Locality 1	395345	6895998	849	11	Back fracture
Locality 2					Back fracture
Locality 3	395413	6896009	833	13	Extensometer 2
Locality 4	395501	6895997	657		Back fracture
Locality 5	395376	6896024	841	12	Extensometer 1
Locality 6	395453	6896009	781 (793)	12	Extensometer 3
Locality 7	395527	6895979	751	10	Extensometer 4
Locality 8	395543	6895977	730	16	Back fracture
Locality 9	395567	6895973	716	6	Back fracture
Locality 10	395614	6895976	711	7	Extensometer 5
Locality 11	395617	6895729	566	12	Middle drill site
Locality 12	395650	6895720	546	11	Middle drill site
Locality 13	395283	6895701	611	24	Total station no. 17
Locality 14	395264	6895666	569	30	Western tape extensometer
Locality 15	395336	6895604	525	16	1962 rockslide
Locality 16	395794	6895647	473	8	“Hoggormtoppen”
Locality 17	395759	6895781	526	20	“Hoggormtoppen”
Locality 18	395335	6896008	812	30	Graben
Locality 19	395553	6895924	686	14	Below extensometer 4 and 5
Locality 20	395646	6895961	667	17	Below extensometer 5
Locality 21	395854	6895301	235	6	Chapel
Locality 22	395821	6895249	192	11	Between the Chapel and the Cathedral
Locality 23	395743	6895199	185	11	Cathedral
Locality 24	395703	6895159	173	19	West of the Cathedral
Locality 25	395509	6895147	192	38	Western Boundary Zone
Locality 26	395805	6895831	544	37	
Locality 27	396093	6895805	445	13	East of Eastern Boundary Zone
Locality 28	395869	6895676	456	35	Eastern Boundary Zone
Locality 29	395862	6895617	414	41	Eastern Boundary Zone
Locality 30	395900	6895400	275		The Cave
Locality 31	395195	6896160	998	15	North of the Back Scarp Zone
Locality 32	395232	6896255	997	16	North of the Back Scarp Zone
Locality 33	395939	6895990	578	22	East of Eastern Boundary Zone
Locality 34	396131	6895735	377	30	East of Eastern Boundary Zone
Locality 35	395525	6895739	595	23	Middle drill site